

# Chapter 1

## Micro and Nano Structural Characterization of SiC

Narendraraj Chandran, Ariadne Andreadou, Alkyoni Mantzari,  
Maya Marinova and Efstathios K. Polychroniadis

**Abstract** For the last decades, substantial research has been focused on the development of Silicon Carbide electronic devices thanks to its outperformance over Silicon. A review of the author's recent results on the microstructure of SiC layers studied by Transmission Electron Microscopy is presented in the current work. Structural defects appearing in epilayers grown by different methods will be presented. The studied samples were grown by different means-from vapour phase techniques such as Physical Vapour Transport, Chemical Vapour Deposition and Sublimation Epitaxy.

### 1.1 Introduction

Due to a wide bandgap energy, high-saturation electron velocity, high breakdown field and high thermal conductivity, Silicon carbide (SiC)-based electronics are suitable for high-power and high frequency applications, as well as for severe environments, including high temperature and high radiation [1]. The large Si–C binding energy (about 5.0 eV) makes it intrinsically resistant to radiation fields, high temperature

---

N. Chandran (✉) · A. Andreadou · A. Mantzari · E. K. Polychroniadis  
Department of Physics, Aristotle University of Thessaloniki, GR54124 Thessaloniki, Greece  
e-mail: naren@physics.auth.gr

A. Andreadou  
e-mail: aria@auth.gr

A. Mantzari  
e-mail: am@auth.gr

E. K. Polychroniadis  
e-mail: polychr@auth.gr

M. Marinova  
Laboratoire de Physique des Solides, Université Paris Sud, Bât 510, 91405 Orsay, France  
e-mail: maya.marinova-atanassova@u-psud.fr

and corrosion. Moreover, because of its high thermal conductivity, it constitutes an excellent heat sink. The combination of such excellent thermal, electrical and mechanical properties makes it also an interesting material for sensor applications in non-standard environmental conditions [2].

SiC crystallizes in many different forms, called polytypes, which differ only in the successive stacking of  $n$  elemental Si–C bilayers. Since they have different bandgap energies and near band edge electronic structures, they should allow the design of new hetero-polytypic devices with unique optical and electrical properties. Unfortunately, up to now, only two SiC polytypes have a well-defined application field. They are hexagonal 4H-SiC for active electronic device layers and 6H-SiC as substrate for Group III–nitride optoelectronics. In this paper, we have studied different SiC polytypes, such as 15R-SiC, 4H-SiC and 3C-SiC, all grown by vapor based growth techniques namely physical vapor transport (PVT), chemical vapor deposition (CVD) and sublimation epitaxy (SE).

15R-SiC has been an attractive material for decades followed by 4H-SiC, and 6H-SiC as a potential candidate for MOS devices [3]. However, no bulk 15R-SiC crystals of good quality have ever been reported. Polytype inclusions and extended defects are the major concerns for crystal growth. In the current study, polytypic transitions were observed during bulk growth. We mainly focused on the interface and formation of associated defects.

Incorporation of group III and IV elements in SiC made astonishing progress in modern power generation technology which requires better semiconductor devices that are capable of operating at higher temperature and at high frequency radiations [4]. Ge and B show relatively high solubility of  $3.8 \times 10^{20} \text{ cm}^{-3}$  and  $1.9 \times 10^{20} \text{ cm}^{-3}$  by replacing Si atoms at 2500 K in SiC [5]. However these results differ in experimental studies depending on the growth technique and temperature. In our case Ge was added as a dopant during CVD 4H-SiC growth.

3C-SiC is regarded advantageous over the other hexagonal polytypes because it shows the highest electron mobility [6] and lower density of the near-interface-traps in the  $\text{SiO}_2/3\text{C-SiC}$  system due to the smaller band gap. A crucial problem hindering the future development of a 3C-SiC technology is the unavailability of 3C-SiC substrates. Frequently, in order to overcome problems related to mismatch, as in the case of Si, the growth is performed on substrates from a hexagonal polytype (4H- or 6H-SiC). In our case, 3C-SiC nucleates spontaneously, during SE growth, on (0001) 6H-SiC surfaces or grows homoepitaxially on 3C-SiC buffer layers priority grown by Vapor-Liquid-Solid (VLS) mechanism.

In all above cases cross-sectional Transmission Electron Microscopy (XTEM) as well as High Resolution Transmission Electron Microscopy (HRTEM) study was performed to gain information on the nano-structural quality of the materials and their defects.

## 1.2 15R-SiC Grown by Physical Vapor Transport

15R-SiC seeds were used to grow single crystals by PVT method. C face  $3^\circ$  off-axis and Si face on-axis seeds were employed. Common growth conditions were applied, i.e.  $2200^\circ\text{C}$  for the growth temperature and a pressure comprised within a range of 15–20 mbar. The thickness of the grown crystals was around 3 mm and the polytype was determined by Raman Spectroscopy. A mixture of 15R/4H-SiC and 15R/6H-SiC crystals were obtained on C-face and Si-face seeds respectively. The main defects observed were stacking faults (SFs) quite abundant in 15R-SiC and normal to [0001] direction. Apart from SFs, a high density of dislocations (D) was observed such as Screw Dislocations (SD), Threading Screw Dislocations (TSD), Threading Edge Dislocations (TED) and Basal Plane Dislocations (BPD). Their density was found to be higher in 15R-SiC area compared to 4H-SiC and 6H-SiC inclusions. Few TEDs and BPDs are identified in TEM images due its well-known conversion mechanism and nature of propagation. Threading dislocations are often introduced at the initial stage of growth and propagate along c-axis and normally terminate or convert into either SFs or BPDs [7].

Polytype transitions depend on various factors such as seed polytype and polarity, supersaturation [3, 8] etc. SiC polytype transitions have been extensively investigated for decades and few authors proposed models for polytypic transition on H-SiC to C-SiC based on asymmetry in the mobility of partial dislocations [9] and 15R-SiC to 6H-SiC based on inhomogeneous density of screw dislocations [10]. On the other hand models are also developed for twins in 15R-SiC such as “Friedelian” reticular merohedric twinning [11]. These studies give better insight for the current study since in case of the C face seeded growth, along with the stacking fault, a (23)/(32) twin sequence was formed in 15R-SiC just below the interface sequence (32)/(22) which is structurally and energetically favored (Fig. 1.1a). This was confirmed by having Fast Fourier Transform (FFT’s) images at these regions. Whereas in Si face seeded growth the polytype transition is more complex due to high SF density (Fig. 1.2b). This implies that twin associated polytype transition is coherent than the other form. Further detailed study is required to extract conclusions on the impact of twins in polytypic transition.

## 1.3 Formation of Ge Droplets on 4H-SiC by Chemical Vapor Transport

Epitaxial 4H-SiC growth was performed at  $1500^\circ\text{C}$  on Si face  $8^\circ$  off-axis 4H-SiC seeds. 0.02 sccm  $\text{GeH}_4$  was added to the  $\text{SiH}_4 + \text{C}_3\text{H}_8$  precursors’ mixture during the deposition run. Ge droplets formed on surface by accumulation of non-incorporated Ge atoms during cooling process.

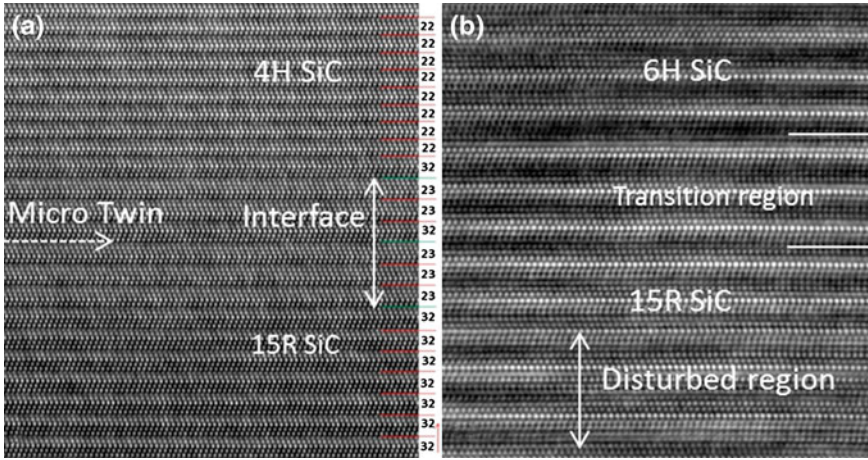


**Fig. 1.1** **a** filtered HRTEM micrograph showing a coherent transition region between 15R-SiC and 4H-SiC interface with alternating (32)/(23) transforming to (32)/(22) atomic sequence. The Zhdanov notation of the stacking sequence, listed at *right*, was measured as indicated by the *arrow*. **b** HRTEM micrograph of 15R-SiC/6H-SiC interface appearing more complex with an extent transition region due the presence of numerous stacking faults

HRTEM was employed to investigate the Ge droplets (Fig. 1.2a) due to recent research on the growth of low-dimensional Ge islands on SiC with an increasing interest to develop optoelectronic SiC devices [12, 13]. The droplets were polycrystalline and their size varied between 20 and 300 nm. Nano-crystallites within the droplets ranged from 5 to 15 nm or in some cases even smaller.

Nano-crystallites were oriented in different directions forming droplets on 4H-SiC. The samples are imaged in two different zone axes i.e. SiC [11-20] (Fig. 1.2a, b) and SiC [1-100] (Fig. 1.2c, d) in order to establish the epitaxial relation. HRTEM micrograph of Fig. 1.2b shows a Ge nano-crystal oriented along  $\text{Ge}\{001\} // 4\text{H-SiC}\{0001\}$ . At the SiC/Ge interface few atomic layers exhibited higher contrast due to atom exchange. The epitaxial orientation of atomic layers was not very clear in SiC [11-20] zone direction. In SiC[1-100] zone direction, it was evident that most of Ge crystals were oriented along  $\text{Ge}\{111\} // \text{SiC}\{0001\}$  direction with few misfit dislocations due to large lattice mismatch of about 30% (Fig. 1.2d). However the step structure of off-axis substrate favored the epitaxial growth considerably reducing the lattice mismatch. TEM characterization at the interface region showed that Ge islands can be grown at low temperature on off axis SiC substrates. Moreover, no Ge inclusions have been detected within the layer.

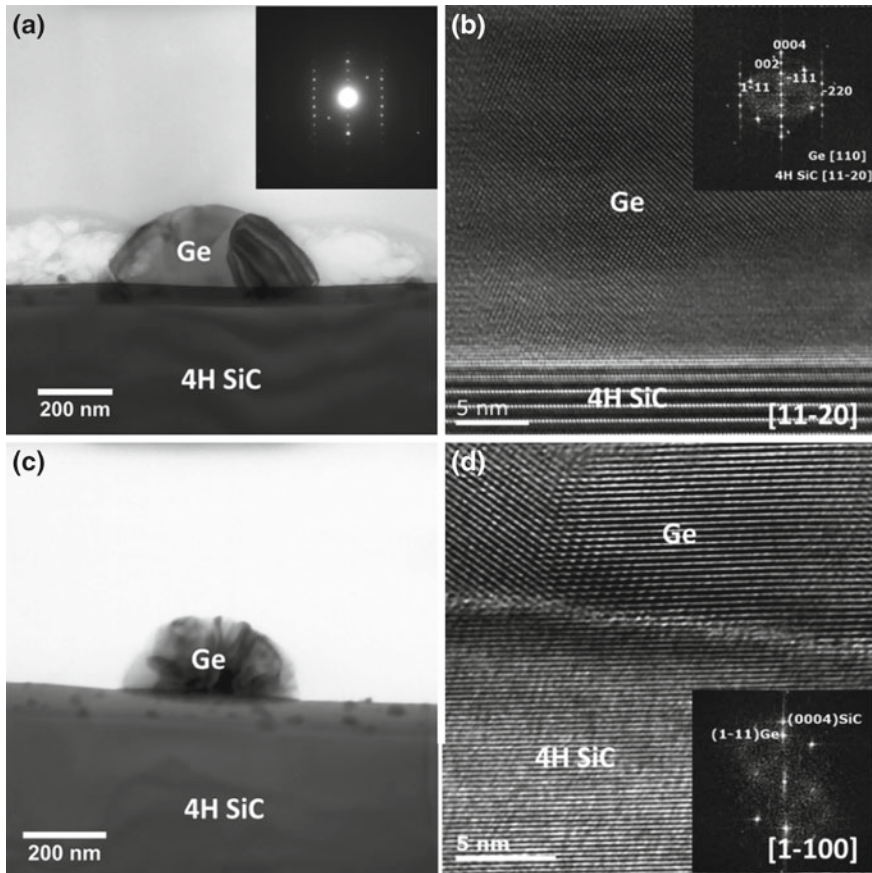


**Fig. 1.2** **a** Low Magnification TEM micrograph along  $[11-20]$  zone direction and **b** HRTEM micrograph and corresponding FFT (insert) revealing the epitaxial growth of Ge  $\{002\}$ // 4H-SiC  $\{0004\}$ . Low magnification and HRTEM micrograph **c**, **d** along  $[1-100]$  zone direction showing that the SiC off-axis step structure favored the epitaxial growth of Ge  $\{1-11\}$  // SiC  $\{0001\}$

## 1.4 3C-SiC Grown by Sublimation Epitaxy

In this case one set of samples was grown on the Si-face of 6H-SiC on-axis substrates in vacuum conditions for 30 min at a temperature of 2000 °C and the temperature gradient ranged from 5 to 8 °C/mm [14, 15] and another set was grown at a source temperature of 1775 °C on differently treated prior growth substrates (e.g. as-received by supplier on-axis, Si-face 6H-SiC substrates, additionally polished 6H-SiC substrates or subjected to a deposition of  $\sim 1.5 \mu\text{m}$  (111) 3C-SiC buffer layer, grown by the VLS mechanism) [16]. A general observation concerning the growth on 6H-SiC substrates by SE is that the 3C-SiC epilayer/substrate interface was not always abrupt. During the initial ramp up the growth can continue by competition

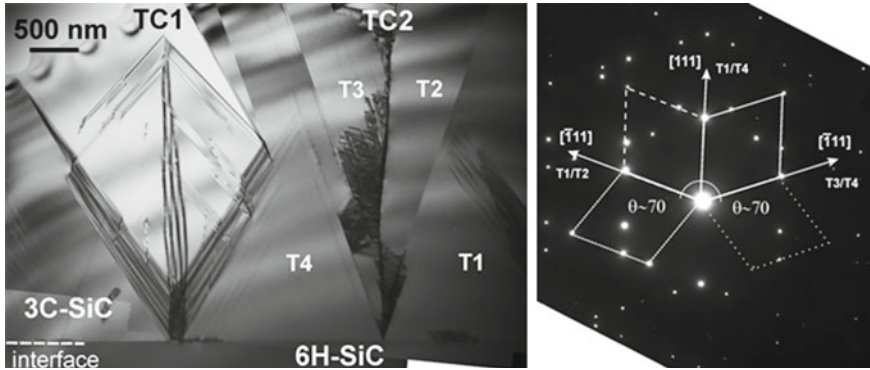


**Fig. 1.3** **a** the formation of fourfold twin structures with nucleation cores on the interface with the 6H-SiC and **b** the corresponding SADP, revealing the relation between the multiple twins

between 3C-SiC heteroepitaxial and 6H-SiC homoepitaxial growth. In some cases a transition zone between the 3C-SiC layer and the 6H-SiC substrate was formed where polytypic transformations occurred through admixture of 15R-SiC, 6H-SiC, 3C-SiC and other irregular stacking sequences [16]. However, in the layers grown when a (111) 3C-SiC buffer layer was deposited before SE, such transformations on the 3C-/6H-SiC interface did not occur.

Typical defects appearing in the layers grown on 6H-SiC substrates, apart from SFs and dislocations, were twins and mainly characteristic triangular defects which are fourfold twin complexes (TC) as shown in Fig. 1.3a. These twin structures have their nucleation cores at the substrate/overgrown interface and once formed they propagate through the whole layer terminating on the surface. When the growth temperature is  $\sim 2000^\circ\text{C}$  [15] and close to the interface with the 6H-SiC they appeared in their simplest form. The analysis of the selected area diffraction pattern (SADP) given in Fig. 1.3b shows that the defect TC2 consists of four grains—two of them twinned along the (111) planes without having a common plane (T1 and T4) and another two (T2 and T3) twinned along the  $(\bar{1}\bar{1}\bar{1})$  planes of T1 and T4, forming two coherent  $\Sigma_3$  interfaces (T1/T2 and T3/T4). Consequently the T2/T3 couple is bounded by one  $\Sigma_{27}$  interface. It is reasonable to assume that the twin complex denoted as TC1 in Fig. 1.3a consists of twins along the  $(1\bar{1}\bar{1})$  and  $(11\bar{1})$  planes. Regarding growth performed at lower temperature and/or on 3C-SiC VLS seeds the complexity of the twinning increases. It is accompanied by formation of other high angle boundaries associated with mis-orientation along the  $[0\bar{1}1]$  [16].

The alteration of temperature gradients affects the crystalline quality of overgrown layers in two ways. First, by lowering the temperature gradient the amount of 6H-SiC in the layer increases. Detailed analysis of the structure of the observed different 3C-/6H-SiC transformation interfaces can be found in [17]. Second, the lowering of the temperature gradient favours strongly the reduction of SFs in the grown 3C-SiC domains [15].

## 1.5 Conclusions

Due to its structural qualities, SiC appears particularly interesting from a crystallographic as well as structural defects point of view. At the same time, the above characteristics affect its growth by making it considerably difficult at certain cases. To make an improvement on the wafer technology, in this work, we investigated SiC crystals grown by three different vapor phase methods. Thus, Physical Vapor Transport (PVT), Chemical Vapor Deposition (CVD) and Sublimation Epitaxy (SE) were used for growing 15R-SiC, Ge doped 4H-SiC and 3C-SiC crystals respectively.

PVT grown 15R-SiC suffers with high order defect density. The planar defects affect the main SiC polytype, which are purely depended on stacking fault formation energies. This fact suggest that may be higher energy is required to form micro-twins which are observed near 15R-SiC/4H-SiC interface. TEM investigation on Ge doped 4H-SiC revealed that CVD technique can be considered suitable growth method for Ge Islands. Growth direction SiC{0001}//Ge {111} found to be the preferred one while the off-axis SiC substrate seems to have favored the epitaxial growth. In case of 3C-SiC layers grown by SE, apart from the typical stacking faults and dislocations some characteristic fourfold twin complexes appeared. Additionally, the thermal gradient decrease led to significant lower stacking fault density but higher amount of 6H-SiC overgrown.

**Acknowledgments** This work was supported by the European Commission through the NetFISiC and MANSiC projects (Grant no. PITN-GA-2010-264613 and Grant no. MRTN-CT-2006-035735). The authors would like to thank Dr. M. Syväjärvi and professor R. Yakimova from the Department of Physics, Chemistry and Biology in Linköping University, Dr. G. Ferro from Laboratoire des Multi-matériaux et Interfaces in Claude Bernard University in Lyon and D. Chaussende from Laboratoire des Matériaux et Génie, INPG Grenoble, for providing the samples.

## References

1. J.A. Cooper Jr., Opportunities and technical strategies for silicon carbide device development. *Mater. Sci. Forum* **15**, 389–393 (2002)
2. C.I. Harris, S. Savage, A. Konstantinov, M. Bakowski, P. Ericsson, Progress towards SiC products. *Appl. Surf. Sci.* **184**, 393 (2001)
3. N. Schulze, D. Barrett, G. Pensl, Controlled growth of 15R-SiC single crystals by the modified Lely method. *Phys. Status Solidi A* **178**(2), 645 (2000)
4. T. Kups, M. Voelskow, W. Skorupa, M. Soueidan, G. Ferro, J. Pezoldt, Lattice location determination of Ge in SiC by ALCHEMI, in *Microscopy of Semiconducting Materials 2007*, vol. 120 (2008), pp. 353–358
5. S.A. Reshanov, I.I. Parfenova, V.P. Rastegaev, Group III-V impurities in  $\beta$ -SiC: lattice distortions and solubility. *Diamond Relat. Mater.* 1278–1282 (2001)
6. M. Bhatnagar, B.J. Baliga, Comparison of 6H-SiC, 3C-SiC, and Si for power devices. *IEEE Trans. Devices* **40**, 645 (1993)
7. S. Chung, V. Wheeler, R. Myers-Ward, C.R. Eddy, D.K. Gaskill, P. Wu, Y.N. Picard, M. Skowronski, Direct observation of basal-plane to threading-edge dislocation conversion in 4H-SiC epitaxy. *J. Appl. Phys.* **109**(9), 094906 (2011)

8. L. Barrett Donovan, N. Schulze, G. Pensl, S. Rohmfeld, M. Hundhausen, Near-thermal equilibrium growth of SiC by physical vapor transport. *Mater. Sci. Eng.* **44**, B61–62 (1999)
9. P. Pirouz, J.W. Yang, Polytypic transformations in SiC: the role of TEM. *Ultramicroscopy* **51**(1), 189 (1993)
10. Yu. Zhang, Chen Hui, Choi Gloria, Raghothamachar Balaji, Dudley Michael, H. Edgar James, K. Grasz, E. Tymicki, L. Zhang, D. Su, Y. Zhu, Nucleation mechanism of 6H-SiC polytype inclusions inside 15R-SiC crystals. *J. Electron. Mater.* **39**(6), 799 (2010)
11. G. Agrosì, G.C. Capitani, E. Scandale, G. Tempesta, Near-atomic images of interfaces between twin-related lamellae in a synthetic 6H-SiC sample. *Phys. Chem. Miner.* **38**(2), 101 (2010)
12. B. Schröter, K. Komlev, U. Kaiser, G. Hess, G. Kipshidze, W. Richter, Germanium on SiC (0001): surface structure and nanocrystals. *Mater. Sci. Forum* **247**, 353–356 (2001)
13. K. Ait-Mansour, D. Dentel, L. Kubler, M. Diani, J.L. Bischoff, D. Bolmont, Epitaxy relationships between Ge-islands and SiC(0001). *Appl. Surf. Sci.* **241**, 403 (2005)
14. M. Beshkova, M. Syväjärvi, R. Vasiliauskas, J. Birch, R. Yakimova, Structural properties of 3C-SiC grown by sublimation epitaxy. *Mater. Sci. Forum* **181**, 615–617 (2009)
15. M. Marinova, A. Mantzari, M. Beshkova, M. Syväjärvi, R. Yakimova, E.K. Polychroniadis, the influence of the temperature gradient on the defect structure of 3C-SiC grown heteroepitaxially on 6H-SiC by sublimation epitaxy. *Mater. Sci. Forum* 645–648, 367–370 (2010)
16. R. Vasiliauskas, M. Marinova, M. Syväjärvi, A. Mantzari, A. Andreadou, J. Lorenzzi, G. Ferro, E.K. Polychroniadis, R. Yakimova, Sublimation growth and structural characterization of 3C-SiC on hexagonal and cubic SiC seeds. *Mater. Sci. Forum* 645–648, 175–178 (2010)
17. M. Marinova, A. Mantzari, M. Beshkova, M. Syväjärvi, R. Yakimova, E.K. Polychroniadis, TEM investigation of the 3C/6H-SiC transformation interface in layers grown by sublimation epitaxy. *Solid State Phenomena* **163**, 97–100 (2010)